

Effects of nanoimprinted patterns in tissue-culture polystyrene on cell behavior

W. Hu^{a)}

Solid State Electronics Laboratory, Department of Electrical Engineering and Computer Science,
The University of Michigan, Ann Arbor, Michigan 48109

E. K. F. Yim

Department of Biomedical Engineering, Johns Hopkins School of Medicine, Baltimore, Maryland 21205

R. M. Reano^{b)}

Solid State Electronics Laboratory, Department of Electrical Engineering and Computer Science,
The University of Michigan, Ann Arbor, Michigan 48109

K. W. Leong

Department of Biomedical Engineering, Johns Hopkins School of Medicine, Baltimore, Maryland 21205

S. W. Pang^{c)}

Solid State Electronics Laboratory, Department of Electrical Engineering and Computer Science,
The University of Michigan, Ann Arbor, Michigan 48109

(Received 1 June 2005; accepted 19 September 2005; published 5 December 2005)

Tissue engineering seeks to develop functional tissues in a biomimetic environment *in vitro*. As the extracellular environment *in vivo* is composed of numerous nanostructures, fabrication of nanostructured substrates will be valuable for tissue engineering applications. In this article, we report a simple nanoimprint lithography (NIL) process to pattern nanostructures directly on tissue-culture polystyrene plates. By repeating this NIL process, three-dimensional scaffolds consisting of multiple-layer nanostructures were also fabricated. Bovine pulmonary artery smooth muscle cells were cultured on imprinted gratings ranging from 350 nm to 10 μm . The smooth muscle cells attached and proliferated well on these imprinted substrates without additional surface treatment. Cell elongation and alignment were observed on the micro- and nanopatterns, with the effect significantly more pronounced on the nanostructures. © 2005 American Vacuum Society.

[DOI: 10.1116/1.2121729]

I. INTRODUCTION

The field of tissue engineering has become one of the main research interests of modern biotechnology. In coaxing the seeded cells to develop into functional tissues, tissue engineering ideally should provide a culture microenvironment that mimics the extracellular matrix (ECM). Extracellular microenvironment is composed of numerous topographical features at the nanoscale, such as nanopores, fibers, ridges, and bands.^{1,2} A better understanding of the cell-substratum interaction on the nanometer scale is crucial to the design of advanced medical devices. There are reports describing cell responses to various materials with micrometer- and nanometer-topography.³⁻⁶ However, the option of producing nanoscale patterns on biomedically-relevant surfaces is limited. Moreover, the significance of nanoscale pattern over micropattern remains unclear. In this study, we demonstrate the efficient production of nanoscale patterns on tissue-culture polystyrene surface, which is optimized for cell culture, with the nanoimprint lithography (NIL). A systematic

investigation of the cell behaviors on nanoimprinted scaffolds was also carried out to gain insight on cell-substratum interaction at the nanometer scale.

From the fabrication perspective, directed cell growth and tissue regeneration requires cost-effective fabrication methods that are able to build complex three-dimensional (3D) nanoscaffolds over large areas. To this end, many lithographic and nonlithographic patterning methods have been explored, which include soft lithography,^{7,8} microcontact printing,^{9,10} injection molding,¹¹ electron beam lithography,^{12,13} solvent-casting and particle-leaching,¹⁴ microsyringe,¹⁵ and gas foaming.¹⁶ However, many of these approaches such as microcontact and soft lithography are generally suitable only for micropatterning. Electron-beam lithography is capable of sub-10 nm patterning,¹⁷ but its throughput is too low to be practical. Nonlithographic techniques such as solvent casting and gas forming can produce nanostructures, but they tend to have poor pattern controllability. Therefore, none of these techniques satisfy all the requirements of nanoscale resolution, high throughput, reproducibility, low cost, and ability to pattern large areas.

Nanoimprint lithography¹⁸ is a versatile technique which satisfies the above-mentioned requirements. We have recently developed NIL techniques that can produce a wide range of nanostructures, including multilayer 3D polymer

^{a)}Present address: Department of Electrical Engineering, The University of Texas at Dallas, Richardson, TX 75083.

^{b)}Present address: Electrical Engineering and Computer Science Department, The Ohio State University, Columbus, OH 43210.

^{c)}Electronic mail: pang@umich.edu

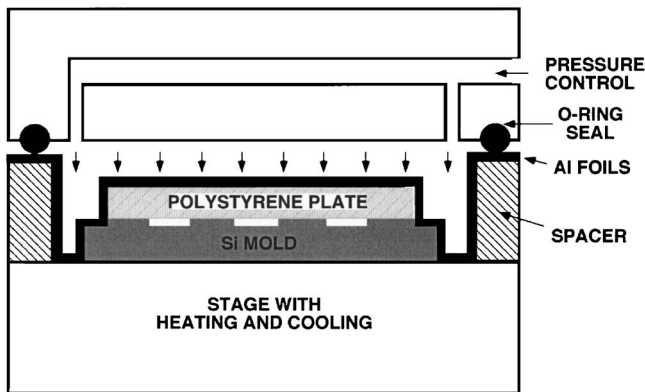


FIG. 1. Configuration of nanoimprint lithography system with tissue-culture polystyrene plates on top of the Si mold.

structures on a Si wafer.^{19–22} Polymers are widely used as biomaterials for tissue engineering because of their potential biocompatibility and biodegradability. Therefore, direct patterning on freestanding polymer films is required. However, conventional NIL is typically used to pattern spin-coated polymer films on supporting substrates and its application to tissue engineering is limited. In this article, we demonstrate a very simple NIL process to pattern thick polymer plates directly as cell-culture dishes. We imprinted directly on the most widely used tissue-culture polystyrene (TCPS) surface with nanoscale resolution. TCPS is commercially surface-treated and optimized for most adherent cell cultures.

Bovine pulmonary artery smooth muscle cells (SMCs) were then cultured on the nanoimprinted patterns and their adhesion and morphology were studied. Our results indicated that nano- and microscale patterns with various heights could be produced with NIL on thick TCPS. SMCs attached and proliferated well on the patterned TCPS without extra surface treatment. Interestingly, the cells aligned and elongated on the patterned TCPS in a size-dependent manner, showing increasing effects as the width of the gratings decreased from 10 μm to 350 nm. In addition, more significant alignment and elongation were observed on gratings with deeper grooves.

Building 3D nanoscaffolds is a major interest in the field of tissue engineering as ECM is 3D in nature and composed of various nanoscale features. Several methods such as electrospinning have been reported for the fabrication of 3D structures.^{13,14,23} However, precise control of nanostructures cannot be achieved using these methods. Motivated by the natural 3D nanostructures on collagens, which has a 400-nm-fibrillar width and 70 nm cross-striation, we have developed a multiple-NIL process to generate similar 3D nanostructures. Using this method, we are able to precisely control the shape, height, width, and pitch of the 3D nanostructures for different cell growth requirements.

II. FABRICATION OF SCAFFOLDS

A. Mold making

Si molds with different nanostructure dimensions were made using lithography and reactive ion etching (RIE). For

the gratings with half-pitch of 70–350 nm, a polymethylmethacrylate (PMMA) film with thickness of 300 nm was spun onto Si wafers and electron beam lithography was performed using a Raith GmbH 150 system at the conditions of 200 pA electron current, 20 μm aperture, 6.5 mm working distance, and accelerate voltage of 20 kV. After lithography, samples were developed in isopropyl alcohol:methyl isobutyl ketone (3:1) for 45 s. Using developed PMMA as the etch mask, the Si molds were etched 200–300 nm deep using Cl_2 in a RIE system, and then the PMMA was removed using hot PRS2000. For the gratings with half-pitch of 500 nm or above, photolithography was performed using an i-line stepper and followed by a similar RIE. After the resist removal by PRS2000 and an O_2 plasma cleaning for 5 min, the molds were treated with 1H,1H,2H,2H-perfluorodecyltrichlorosilane (FDTs) to generate a low-energy surface,²¹ which is critical for mold-polymer separation after NIL.

B. Nanoimprint in polystyrene

Nanostructures with 100 nm–10 μm half-pitch, and 200–900 nm in height in commercial 1.5 mm thick TCPS plates were formed by NIL with the configuration shown in Fig. 1 in an Obducat NIL 4 system. A TCPS plate was placed on the top of a Si mold. For samples or molds that were <4 in. in diameter, 3–8 Al foils were used as the sealing cover across the 4 in. stage. The stage was heated by resistive heating. A pressure of 5–8 MPa and a temperature of 150–180 $^\circ\text{C}$ were applied to the system for about 5–10 min. During imprinting, the TCPS plate was softened and was pressed into the mold underneath. The imprinting temperature was well above the glass transition temperature (T_g) of TCPS ($T_g=95\text{--}105\text{ }^\circ\text{C}$), resulting in a polymer at a viscous fluid state and the TCPS was amenable to molding and flow. After 5–10 min of imprinting at elevated temperature and pressure, the TCPS and the mold were allowed to cool to below the T_g of the TCPS, thereby producing permanent nanostructures that were a replica of the mold patterns on the TCPS plate. The Si mold could be separated from the TCPS plate easily due to the low surface energy resulted from treating the mold with FDTs prior to imprinting.

Figure 2 shows scanning electron micrographs of the TCPS nanostructures imprinted at a temperature of 150 $^\circ\text{C}$ and a pressure of 5 MPa for 10 min. The PS grating in Fig. 2(a) was imprinted with a Si grating mold of 330 nm width, 1 μm pitch, and 450 nm height. Since the PS imprint has the same dimensions as the Si mold, the PS was able to fill the mold completely at these imprint conditions. Figure 2(b) shows a PS grating of 120 nm width, 290 nm height, and 380 nm pitch, which were also similar to the mold. At these imprint conditions, the imprinted gratings were well formed with high uniformity and low defects, and the process is robust for making TCPS scaffolds.

C. 3D scaffolds by multiple imprints

Cells are organized in a 3D manner *in vivo*. Fabrication of 3D scaffolds is therefore of interest to tissue regeneration.

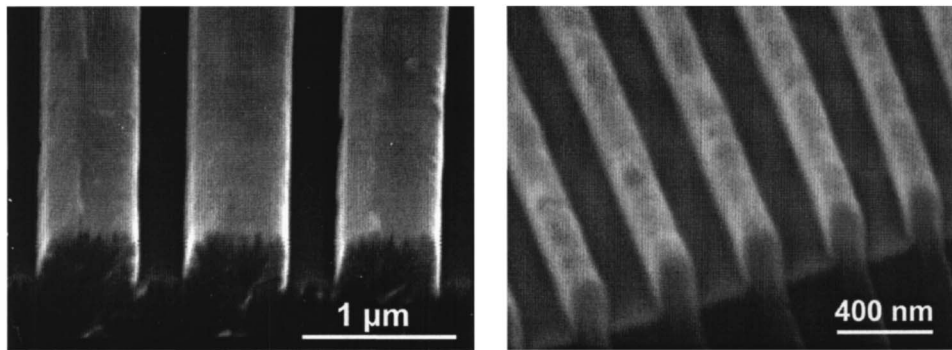


FIG. 2. Nanoimprinted structure in thick tissue-culture polystyrene: (a) gratings with $0.5\ \mu\text{m}$ half-pitch and $440\ \text{nm}$ height and (b) gratings with $120\ \text{nm}$ half-pitch and $290\ \text{nm}$ height.

Recently, it is reported that stacking freestanding polymer thin films patterned by soft lithography can generate 3D scaffolds.⁷ However, this method is mainly useful for micrometer structures and the controllability of the 3D scaffolds is poor. Here we report a simple method to imprint 3D nanostructures directly on freestanding TCPS plates using multiple NIL process. The first imprint was a conventional NIL as discussed in the previous section. The second imprint used the same setup as shown in Fig. 1, however we had to reduce the imprint temperature or pressure so that the second layer of the imprinted nanostructures would not perturb the first imprint. Figure 3 shows the 3D nanoscaffolds consisting of $100\ \text{nm}$ gratings embedded on $1\ \mu\text{m}$ wide grating structures fabricated using this method. The first imprint was performed at $150\ ^\circ\text{C}$ and $5\ \text{MPa}$ for $10\ \text{min}$ with a $1\ \mu\text{m}$ half-pitch grating mold of $680\ \text{nm}$ height. The second imprint was performed at $85\ ^\circ\text{C}$ and $5\ \text{MPa}$ for $10\ \text{min}$ with a $100\ \text{nm}$ wide grating mold of $300\ \text{nm}$ height. The heights of the first imprinted grating (bottom layer) and the second imprinted grating (top layer) were $650\ \text{nm}$ and $45\ \text{nm}$, respectively. Both layers can be any size or shape such as dots, circles, squares, and gratings. The layers can be aligned to each other or offset at any angle. Figures 3(a) and 3(b) show two structures with the top layer of gratings aligned perpendicular and parallel to the bottom layer. The alignment accuracy is similar to the optical aligner when transparent molds are used and is determined by the imprint system alignment capability. With proper alignment setup, submicrometer alignment accuracy is achievable. Therefore, this multiple imprint technique offers the unique flexibility for 3D pattern

design and fabrication to satisfy various cell-growth requirements.

Another advantage of the multiple-NIL technique is the high controllability of 3D nanostructures. By choosing different NIL temperature and pressure, we can control the imprint heights of both the bottom and top layers. Figure 4 shows how the pattern heights vary with the imprint temperature and pressure. The bottom layers were imprinted at the same conditions and mold as Fig. 3. For Fig. 4(a), the top layer was imprinted at a fixed pressure of $5\ \text{MPa}$ and varying temperature of $70\text{--}150\ ^\circ\text{C}$. For Fig. 4(b), the top layer was imprinted at a fixed temperature of $85\ ^\circ\text{C}$ and varying pressure of $2.0\text{--}6.5\ \text{MPa}$. The heights of the bottom and top layers were measured using an atomic force microscope. As shown in Fig. 4(a), with the imprint pressure fixed at $5\ \text{MPa}$, the height of the bottom grating decreases monotonically with the increased temperature, while the height of the top grating increases. During the second imprint of the top grating, the viscosity of polystyrene decreases with increasing temperature, resulting in polymer flow and bottom grating height decreases with increasing temperature. At $115\ ^\circ\text{C}$, which is $20\ ^\circ\text{C}$ above the glass transition temperature of TCPS, the height of the bottom grating decreased significantly to $120\ \text{nm}$. The lateral feature size of the bottom grating also changes due to polymer flow. Therefore, the imprint temperature for 3D nanostructures is chosen to be $85\ ^\circ\text{C}$ to minimize the effects of the second imprint on the bottom grating. Imprint pressure also affects the flow of polymer as shown in Fig. 4(b). The imprint temperature is fixed at $85\ ^\circ\text{C}$. The height of the top grating increases and the bot-

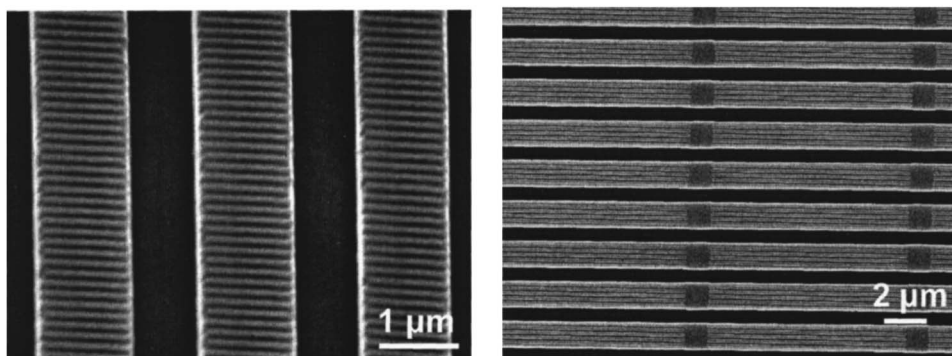


FIG. 3. 3D polystyrene nanostructures with multiple imprints: 100-nm -wide gratings imprinted on $1\ \mu\text{m}$ half-pitch gratings with (a) perpendicular orientation (view at 45°) and (b) parallel orientation (top view).

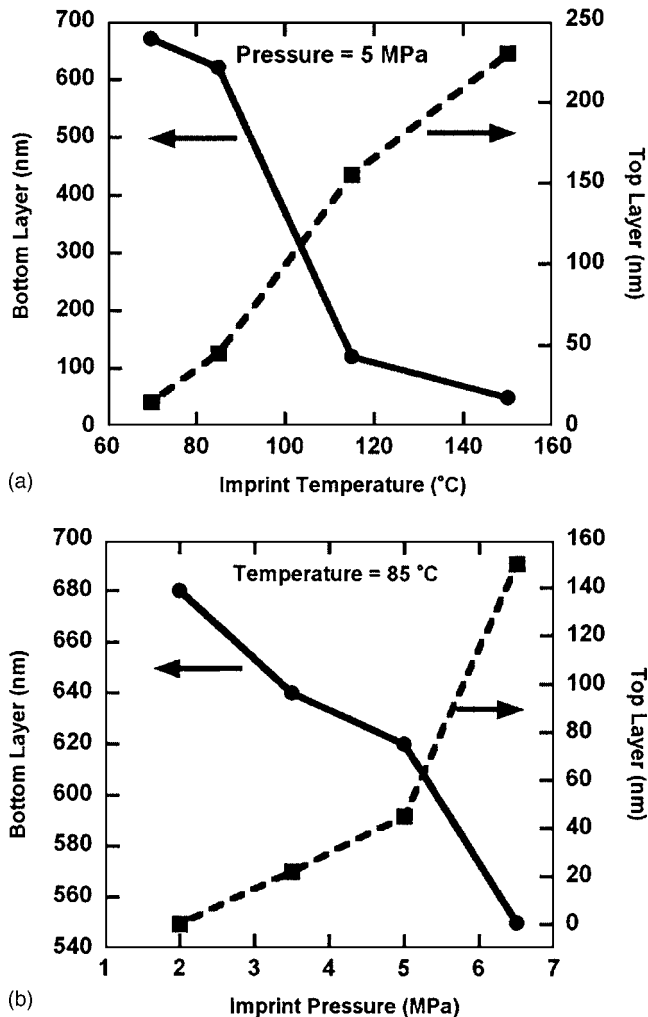


Fig. 4. Heights of the bottom and top layer with multiple imprints, as a function of the second-imprint (a) temperature when the imprint pressure was fixed at 5 MPa and (b) pressure when the imprint temperature was fixed at 85 °C.

tom grating height decreases monotonically with the increase of imprint pressure. The changes in the height and lateral feature size of the top and bottom gratings are controllable and they can be taken into account as design biases. By adjusting the imprint conditions and the mold dimensions, 3D nanostructures with various features and heights can be obtained.

III. CELL BEHAVIOR ON IMPRINTED STRUCTURES

After the imprinted scaffolds were made, the same number of bovine pulmonary artery SMCs were cultured on the nanoimprinted TCPS plates and their alignment and morphology were studied using fluorescence microscopy. Figure 5 shows the confocal micrographs of SMCs on unpatterned and patterned TCPS plates. Note that the underlying PS gratings were not visible in the fluorescence images. Bovine pulmonary artery SMC were obtained from Cambrex (Walkersville, MD) and seeded on the micro- or nanoimprinted TCPS at 50×10^3 cell/cm². Precut unpatterned TCPS was used as controls. Samples were fixed in 4% paraformaldehyde and

permeabilized with 0.05% Triton-X and 50 mM glycine solution. The F-actin was stained with Oregon Green 488 phalloidin (Molecular Probes, OR), and the nucleus was stained with DAPI (Molecular Probes, CA). Samples were thoroughly washed with phosphate buffered saline before inspection with confocal microscopy. Smooth muscle cells exist in various phenotypes *in vivo*, which change in response to changes in their environment. For example, in the tunica media layer of artery, SMCs are aligned circumferentially, with an elongated morphology. However, cell morphology changes during vascular morphogenesis and upon isolation for *in vitro* culture. The physiology of SMCs is extensively reviewed by Owen and co-workers.²⁴ For the cell study, the number of cells seeded on each sample was the same. However, the cell distribution was not even, with higher- and low-density areas. Micrographs were taken from random areas, some with higher density and some with lower density, but a fixed number of 300 cells was counted for the analysis shown in the Figs. 6 and 7. In Fig. 5(a), the direction of SMCs on unpatterned TCPS plate was random and no cell elongation was observed. Cells show obvious alignment and elongation on the 2 μm [Fig. 5(b)], 1 μm [Fig. 5(c)], and 0.5 μm [Fig. 5(d)] half-pitch TCPS gratings. In addition, the nuclei were also elongated and aligned. Such results indicate that the imprinted micrometer and nanometer scale structures have strong influence on cell morphology. Moreover, the alignment and elongation on the 0.5 μm [Fig. 5(d)] half-pitch TCPS gratings were more significant than the 1 μm [Fig. 5(b)] and 2 μm [Fig. 5(c)] gratings.

To study the influence of grating width on cellular behavior, quantitative analysis of SMCs alignment and elongation was performed and the results are shown in Fig. 6. The grating height in the TCPS patterns was ~ 300 nm and the half pitch of the gratings was varied from 350 nm to 10 μm . For alignment measurement, cells were considered aligned if the angle between their long axis and the grating was less than 15°. For each grating dimension, an average of 300 cells was counted. The elongation factor ($E = \text{cell long axis/short axis} - 1$) describes the extent the equimomental ellipse is lengthened or stretched out. For example, E for a circle is 0 and E is 1 for an ellipse with an axis ratio of 1:2. 150–200 cells were measured from each sample for elongation evaluation. The results clearly show that the efficiency of SMCs alignment and elongation increases monotonically with the decrease of grating pitch, indicating that nanoscale structures produce more efficient alignment and elongation than micrometer-scale patterns. For example, 350 nm half-pitch gratings yield 92% alignment and an elongation factor of 10.5 while 10 μm gratings yield only 37% alignment and an elongation factor of 4.3. This nonlinear influence trend proves that nanostructures have significant influence on SMC behavior.

Likewise, SMCs alignment and elongation also depend on the height of the imprinted patterns, as shown in Fig. 7. With the grating width in the TCPS patterns fixed at 2 μm , deeper gratings increase cell alignment efficiency. For example, a 2- μm wide grating with an 800-nm height can achieve a

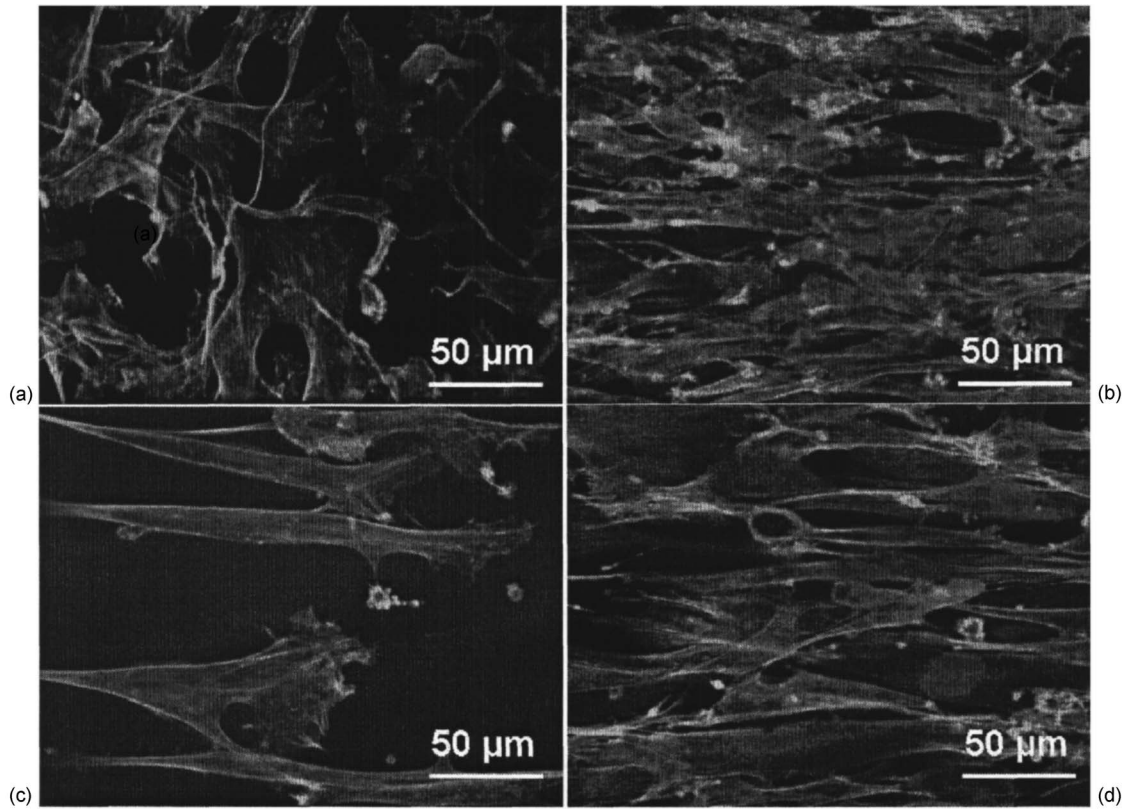


FIG. 5. Fluorescence micrographs of smooth muscle cells on (a) unpatterned TCPS, (b) 2 μm half-pitch gratings, (c) 1 μm half-pitch gratings, and (d) 0.5 μm half-pitch gratings. All gratings are along the horizontal direction.

95% alignment efficiency. The results show that the height is another important controllable factor in the imprinted patterns that can significantly affect cell behavior.

IV. SUMMARY

Building nanoscaffolds which can support and precisely manipulate and guide cells to form functional tissues is a challenge. Towards this endeavor, we applied NIL to pattern the commercial TCPS plates with nanometer precision. Us-

ing multiple NIL process, we demonstrated the fabrication of multiple-layer nanostructures that serve as 3D scaffolds for cell growth. The cell-culture results show that these imprinted polymer scaffolds with nanotopographical features can effectively direct the SMC orientation. The NIL process can be applied to pattern 2D or 3D nanotopography of different geometry on a wide range of polymers including popular biocompatible and biodegradable polymers. Due to its high precision, unique flexibility, good controllability, and

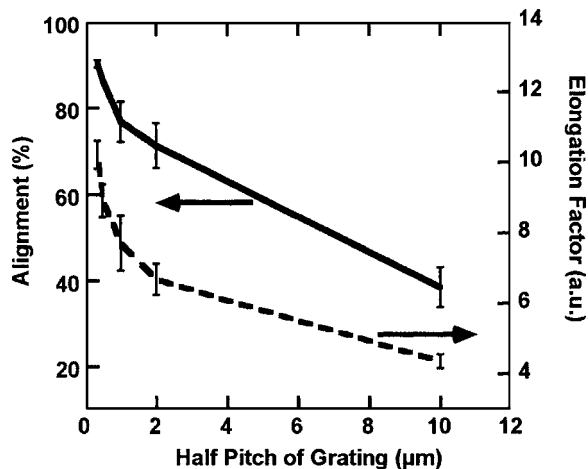


FIG. 6. Alignment and elongation factor of smooth muscle cells as a function of grating width for 300 nm deep gratings.

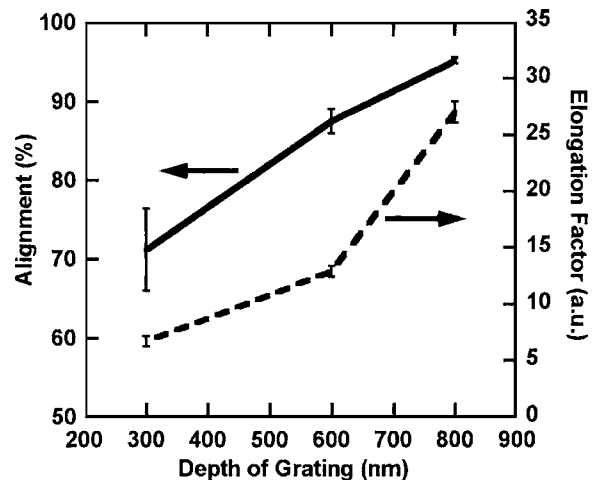


FIG. 7. Effects of the grating height for 2 μm wide polystyrene gratings on the alignment and elongation factor of smooth muscle cells.

high throughput, this NIL technique is suitable for nanoscaffold fabrication for the study of cell-cell and cell-substrate interactions.

ACKNOWLEDGMENT

The authors would like to acknowledge the support of this work by NIH under Grant No. R21EB003203.

- ¹G. A. Abrams, S. L. Goodman, P. F. Nealey, M. Franco, and C. J. Murphy, *Cell Tissue Res.* **299**, 39 (2000).
- ²G. A. Abrams, E. Bentley, P. F. Nealey, and C. J. Murphy, *Cells Tissues Organs* **170**, 251 (2002).
- ³P. Clark, P. Connolly, A. S. Curtis, J. A. Dow, and C. D. Wilkinson, *J. Cell. Sci.* **99**, 73 (1991).
- ⁴A. Curtis and C. Wilkinson, *Biomaterials* **18**, 1573 (1997).
- ⁵A. S. Andersson, F. Backhed, A. von Euler, A. Richter-Dahlfors, D. Sutherland, and B. Kasemo, *Biomaterials* **24**, 3427 (2003).
- ⁶D. C. Miller, A. Thapa, K. M. Haberstroh, and T. J. Webster, *Biomaterials* **25**, 53 (2004).
- ⁷R. S. Kane, S. Takayama, E. Ostuni, D. E. Ingber, and G. M. Whitesides, *Biomaterials* **20**, 2363 (1999).
- ⁸G. Vozzi, C. Flaim, A. Ahluwalia, and S. Bhatia, *Biomaterials* **24**, 2533 (2003).
- ⁹R. J. Jackman, J. L. Wilbur, and G. M. Whitesides, *Science* **269**, 664 (1995).
- ¹⁰S. Brittain, K. Paul, X. M. Zhao, and G. M. Whitesides, *Phys. World* **11**, 31 (1998).
- ¹¹N. Gadegaard, S. Mosler, and N. B. Larsen, *Macromol. Mater. Eng.* **288**, 76 (2003).
- ¹²A. I. Teixeira, G. A. Abrams, C. J. Murphy, and P. F. Nealey, *J. Vac. Sci. Technol. B* **21**, 683 (2003).
- ¹³N. Gadegaard, S. Thoms, D. S. Macintyre, K. Mcghee, J. Gallagher, B. Casey, and C. D. W. Wilkinson, *Microelectron. Eng.* **67**, 162 (2003).
- ¹⁴S. L. Ishaug-Riley, G. M. Crane-Kruger, M. J. Yaszemski, and A. G. Mikos, *Biomaterials* **19**, 1405 (1998).
- ¹⁵G. Vozzi, A. Previti, D. De Rossi, and A. Ahluwalia, *Tissue Eng.* **8**, 1089 (2002).
- ¹⁶J. Mooney, D. F. Baldwin, N. P. Suh, J. P. Vacanti, and R. Langer, *Biomaterials* **17**, 1417 (1996).
- ¹⁷W. Hu, G. H. Bernstein, K. Sarveswaran, and M. Lieberman, *J. Vac. Sci. Technol. B* **22**, 1711 (2004).
- ¹⁸S. Y. Chou, P. R. Krauss, and P. J. Renstrom, *Science* **272**, 85 (1996).
- ¹⁹X. D. Huang, L. R. Bao, X. Cheng, L. J. Guo, S. W. Pang, and A. F. Yee, *J. Vac. Sci. Technol. B* **20**, 2872 (2002).
- ²⁰L. R. Bao, X. Cheng, X. D. Huang, L. J. Guo, S. W. Pang, and A. F. Yee, *J. Vac. Sci. Technol. B* **20**, 2881 (2002).
- ²¹L. Tan, Y. P. Kong, L. R. Bao, X. D. Huang, L. J. Guo, S. W. Pang, and A. F. Yee, *J. Vac. Sci. Technol. B* **21**, 2742 (2003).
- ²²Y. P. Heng, L. Tan, S. W. Pang, and A. F. Yee, *J. Vac. Sci. Technol. A* **22**, 1873 (2004).
- ²³M. Lee, J. C. Y. Dunn, and B. M. Wu, *Biomaterials* **26**, 4281 (2005).
- ²⁴G. K. Owens, M. S. Kumar, and B. R. Wamhoff, *Physiol. Rev.* **84**, 767 (2004).